Letter Vol. 5, No. 4 / April 2018 / Optica 475

optica

Time-dependent population inversion gratings in laser frequency combs

Marco Piccardo,[1] Dmitry Kazakov,[1,2] Noah A. Rubin,[1] Paul Chevalier,[1] Yongrui Wang,[3] Feng Xie,[4] Kevin Lascola,[4] Alexey Belyanin,[3] and Federico Capasso[1,*]

[1]Harvard John A. Paulson School of Engineering and Applied Sciences, Harvard University, Cambridge, Massachusetts 02138, USA
[2]Department of Information Technology and Electrical Engineering, ETH Zurich, 8092 Zurich, Switzerland
[3]Department of Physics and Astronomy, Texas A&M University, College Station, Texas 77843, USA
[4]Thorlabs Quantum Electronics (TQE), Jessup, Maryland 20794, USA
*Corresponding author: capasso@seas.harvard.edu

Received 15 February 2018; revised 21 March 2018; accepted 27 March 2018 (Doc. ID 323413); published 17 April 2018

In standing-wave lasers, spatial hole burning induces a static grating of the population inversion, enabling multimode operation with several independent lasing modes. In the presence of a mode-locking mechanism, these modes may become correlated, giving origin to a frequency comb. Quantum cascade lasers, owing to their ultrafast gain dynamics, are ideally suited to achieve comb operation. Here we experimentally demonstrate that the modes of a quantum cascade laser frequency comb coherently beat to produce time-dependent population inversion gratings, which spatially modulate the current in the device at frequencies equal to the mode separation and its higher harmonics. This phenomenon allows the laser to serve as a phased collection of microwave local oscillators and is utilized to demonstrate quadrature amplitude modulation, a staple of modern communications. These findings may provide for a new class of integrated transmitters, potentially extending from the microwave to the low terahertz band.

OCIS codes: (140.5965) Semiconductor lasers, quantum cascade; (350.4010) Microwaves; (190.4380) Nonlinear optics, four-wave mixing.

https://doi.org/10.1364/OPTICA.5.000475

In a homogeneously broadened standing-wave laser, the first lasing mode arising in the laser will induce, assuming negligible carrier diffusion, a static grating of population inversion with minima corresponding to the antinodes of the mode intensity [Figs. 1(a) and 1(b)] and a period of a half optical wavelength in a process known as spatial hole burning (SHB) [1]. SHB enables mode coupling and multimode operation. Adjacent cavity modes present crests in areas where the population inversion is high [Fig. 1(a)]; these modes are then able to locally extract gain from the medium and begin lasing. The temporal beating among the modes in turn induces a dynamic component in the population grating, oscillating at the beat frequency with a spatially varying amplitude and phase determined by the profiles of the optical standing waves [Fig. 1(c)].

Various studies have focused on the effects of static SHB in semiconductor lasers—mostly distributed feedback (DFB) structures—to investigate the origin of single-mode instabilities, making use of optical techniques that relate the profile of spontaneous emission across the laser to the carrier distribution via the bimolecular recombination rate [2–4]. Dynamic population gratings have been studied in different systems: in DFB lasers, dynamic SHB was created by modulating the drive current of the device with a microwave signal [5], while in bare gain media it was shown that intersecting two tunable laser beams produced a moving population grating oscillating at the frequency difference of the two beams [6,7]. However, despite more than 50 years of studies [8], no direct experimental evidence of the intrinsic dynamic grating originating from the beating of modes in standing-wave lasers has ever been reported. Here we present a conceptually simple microwave measurement capable of probing time-dependent population inversion gratings in quantum cascade laser (QCL) frequency combs. These gratings arise from the coherent beating of longitudinal modes of the laser. The QCL platform is ideal for the observation of such a phenomenon because of its fast gain recovery dynamics associated with the short relaxation times of intersubband transitions [9] (≈ps long), which simultaneously allows high-frequency oscillations of the population inversion (up to a few terahertz) and limits the diffusion of excited carriers to subwavelength distances (typically a few hundred nanometers), preventing the washout of SHB effects [1]. The spatial nature of the dynamic gratings allows the laser to serve as a phased collection of local oscillators at the intermodal beat note frequency. This enables the use of a mid-infrared QCL, not only as a microwave source, but also as a microwave mixer for quadrature amplitude modulation (QAM), a scheme widely used in modern communications.

All the studied devices are continuous wave, buried heterostructure, uncoated Fabry–Perot (FP) QCLs operating in a frequency comb regime in the mid-infrared spectral range (see Section 1 in Supplement 1 for details). Our findings show that the intracavity intermode beat profiles exhibit a universal

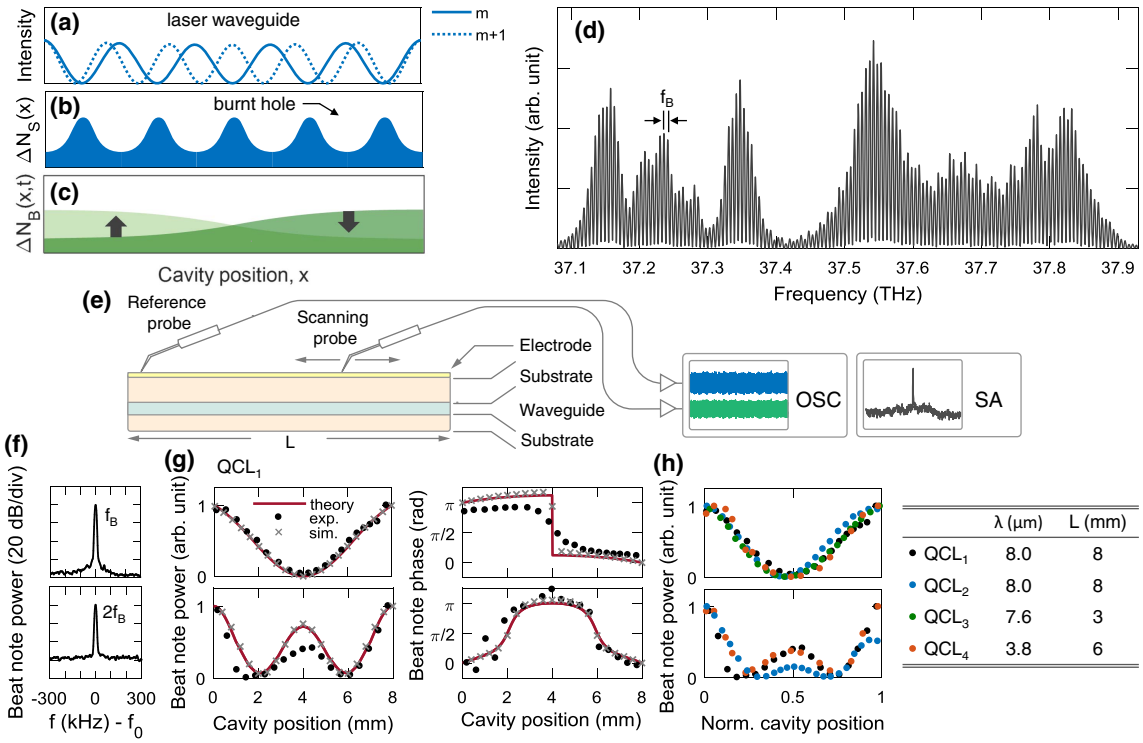

Fig. 1. Mapping time-dependent population inversion gratings in QCL combs. (a)–(c) Emergence of inversion grating effects, known as SHB, in a standing-wave laser: an optical mode m starts lasing inside the cavity (a), inducing a static grating ΔN_S (b). This in turn allows another mode $m+1$ to oscillate and beat with the first mode, inducing a dynamic grating ΔN_B that oscillates periodically (c) in the direction indicated by the arrows (two snapshots of such oscillatory grating taken at times differing by half of the oscillation cycle are shown in two shades of green). (d) Measured optical spectrum of QCL_1 operating in a comb regime. (e) Schematic of the setup used for the measurement of intracavity beat profiles in a QCL. Two microwave probes are positioned on the top electrode of the laser with cavity length L. As one probe is scanned across the longitudinal axis of the cavity, the detected signals can be recorded with a digital sampling oscilloscope (OSC) or a microwave spectrum analyzer (SA). (f) Spectra measured on the SA (resolution bandwidth: 1 kHz) of the fundamental ($f_0 = 5.6$ GHz) and second order ($f_0 = 11.2$ GHz) beat notes of QCL_1. (g) Power and phase of the intracavity beat profiles measured on QCL_1 (circles) at f_B (top) and $2f_B$ (bottom). Also shown are the predictions of the analytical model presented in the text (continuous lines, parameters: $L = 8$ mm, $R = 0.28$) and of numerical simulations (crosses). (h) Intracavity beat profiles measured at f_B (top) and $2f_B$ (bottom) on four different devices with emission wavelength and cavity length specified in the table.

signature of the dynamic gratings, which is not affected by the emission wavelength or cavity length of the specific device. We will concentrate our focus in the following on a representative device (QCL_1), for which a full set of studies is presented.

The spectrum of QCL_1 exhibits a large number of modes separated by a beat frequency $f_B = 5.6$ GHz [Fig. 1(d)]. The beat note spectra measured with a spectrum analyzer at f_B and $2f_B$—produced by the intermodal beating of the nearest and second-nearest neighbors, respectively—exhibit a narrow (kilohertz) linewidth [Fig. 1(f)], a typical signature of comb operation [10] (see Section 2 in Supplement 1 for more details). Previous studies have shown that the intermode beat note can be extracted directly off the chip from the QCL as a modulation of the current driving the laser [11,12]; however, no attempts were made to access the spatial dependence of the beat signal across the laser cavity. The measurement of time-dependent population inversion gratings presented here relies on the detection of the amplitude and phase of microwave signals at different positions along the laser cavity. These microwave signals are produced by current modulation inside the laser directly linked to the dynamics of the optical field. A schematic of the experimental setup is shown in Fig. 1(e). Two microwave probes are brought in electrical contact with the top electrode of the operating laser: one is scanned along the longitudinal axis of the cavity using a micrometer positioning stage, while the other is kept at a fixed position to extract a phase-reference signal. The detected signals can be examined using a microwave spectrum analyzer, to study the power spectra of the intermodal beat notes generated inside the cavity, or recorded with a digital sampling oscilloscope, to retrieve the phase of the beat notes (see Section 1 in Supplement 1 for further details). Scanning across the laser cavity, we record beat note power patterns [Fig. 1(g)], whose universal character is supported by their observation in different devices [Fig. 1(h)]. The patterns exhibit antinodes at the edges of the cavity and a number of nodes equal to the order of the intermodal beat note. The corresponding phase profiles show a smooth phase transition between 0 and π at the positions of the power nodes, indicating that adjacent lobes of the power profiles oscillate in antiphase. A series of control experiments based on the injection of external microwave signals excludes the possibility of artifacts in the observed beat profiles due to transmission line effects (Section 4 in Supplement 1).

A simple analytical model accounts for the measured profiles. Its derivation is outlined in Section 6 of Supplement 1. Here we present the underlying reasoning alongside the fundamental result. In a symmetric FP laser with cavity length L, facet reflectivity R, and unsaturated net gain coefficient $g = 1/L \log(1/R)$, the

cavity mode m is in general a partial standing wave characterized by an amplitude A_m, a spectral phase ϕ_m, a wave vector $k_m = \pi m/L$, and an angular frequency $\omega_m = ck_m/n_w$, where n_w is the effective refractive index of the waveguide. The total intracavity field intensity obtained by summing the contributions of all N lasing modes will contain components oscillating at the intermodal beat frequency, inducing a dynamic grating [Fig. 1(c)] in addition to the static SHB component. By expanding the total intracavity intensity in a Fourier series and keeping only slowly varying spatial oscillations (Section 6 in Supplement 1), we obtain that the spatiotemporal dependence of the component oscillating at the nth harmonic of f_B is

$$I_{B,n} = \sum_{m=1}^{N-n} A_m A_{m+n}[\cos(nk_B x + n\omega_B t + \Delta\phi_{m+n,m})e^{-gx} + \cos(nk_B x - n\omega_B t - \Delta\phi_{m+n,m})e^{-g(L-x)}], \quad (1)$$

where k_B and ω_B are determined by the difference of wave vectors and angular frequencies, respectively, of any pair of adjacent modes. By means of stimulated emission and absorption, the spatiotemporal variations of the field intensity described by Eq. (1) directly translate into variations of the population inversion, ultimately modulating the vertical current flowing in the device. It is illuminating to consider the case of a perfect standing-wave cavity ($R = 1$, $g = 0$), in which case Eq. (1) becomes simply

$$I_{B,n} = \sum_{m=1}^{N-n} 2A_m A_{m+n} \cos(nk_B x)\cos(n\omega_B t + \Delta\phi_{m+n,m}), \quad (2)$$

where the standing-wave character of the intensity oscillations is clear. The predictions of the analytical model presented here are shown in Fig. 1(g) and are confirmed by space- and time-domain simulations of transport and recombination in the QCL active region based on coupled density matrix and Maxwell equations [13] (Section 7 in Supplement 1). The similarity with the experimental measurements is evident (Discussion 6E in Supplement 1). The agreement is particularly remarkable in that a macroscopic measurement is capable of probing local oscillations of the population inversion occurring inside a buried waveguide with a lateral dimension of only a few microns. We have also carried out a similar measurement using an FP diode laser ($L = 2.5$ mm) emitting tens of longitudinal modes in the near-infrared range (1.45 μm) with high optical output power (2.5 W), but no beat note could be electrically extracted from the laser. We cannot exclude the possibility that current oscillations are damped in the diode laser chip, but consider it unlikely, given that the chip is similar to that of QCLs. It is more likely that coherent population pulsations mediated by four-wave mixing interactions in the gain medium are much stronger in the QCL as compared to the diode laser.

This view of the beat note—as a spatially varying quantity—provides for novel laser applications in which the laser is not used as a source of optical radiation but rather as a microwave source that essentially amounts to an array of phase-coherent oscillators. In particular, we show that this allows the laser to act as a quadrature mixer, imbuing it with a new, unconventional functionality. QAM is a technique used extensively in modern telecommunication systems. Due to the fact that both amplitude and phase of the carrier are modulated, it allows for doubling the spectral efficiency of the transmitted signal. This is achieved by combining two amplitude-modulated carriers in a single physical channel exploiting the orthogonality of trigonometric functions [14]. A block diagram of a quadrature mixer is shown in Fig. 2(a). Two baseband signals $I(t)$ and $Q(t)$ are mixed, respectively, with the carrier wave and its copy delayed by 90°, producing the in-phase and quadrature modulated carriers, that, after subsequent summation, yield a QAM waveform. A proof-of-principle demonstration of a QCL operating as a microwave quadrature mixer is illustrated in Figs. 2(b)–2(d) (see Methods for further details). We pick the fundamental beat note at 5.6 GHz as a carrier for QAM. This choice is, by all means, arbitrary and QAM could be done with beat notes of any order, the only restriction being the bandwidth of the experimental setup. In our setting the signal-to-noise ratio of the tone at $2f_B$ is on average 20 dB lower than at f_B [cf. Fig. 1(f)] due to the bandwidth limitations of the electronics in use, which motivates the choice of the fundamental beat note for QAM. With the same microwave probes used for the mapping experiment, we apply two tones, $I = 35$ MHz and $Q = 89$ MHz, as modulating signals at positions where the intermodal beat note of the QCL is dephased by 90° [Fig. 2(b)]. The beat note is mixed with the applied microwave tones inside the laser thanks to the diode-like

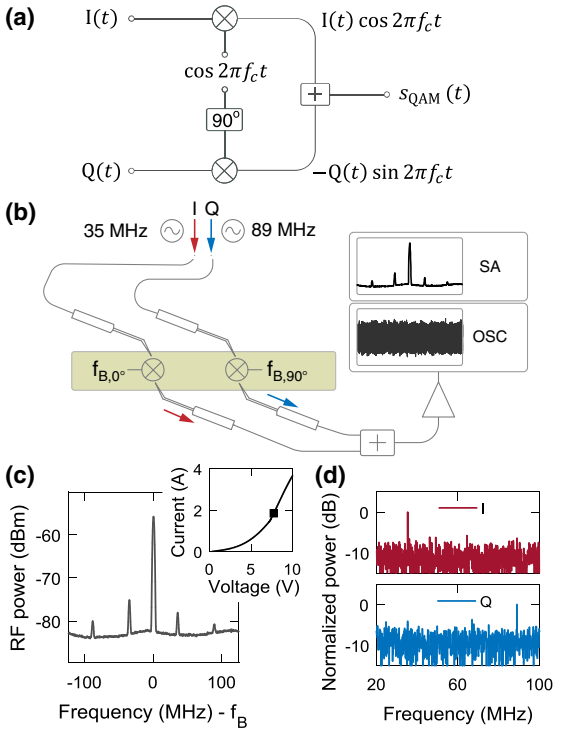

Fig. 2. QCL as a microwave quadrature mixer. (a) Block diagram of a generic quadrature mixer. $I(t)$ and $Q(t)$ are two input baseband signals, f_c is the carrier frequency, s_{QAM} is the QAM waveform. (b) Schematic of the setup used to demonstrate microwave QAM with a QCL comb generator. The rectangular bar is the top view of the laser contact. Two sinusoidal signals are injected and electrically mixed inside the laser with intermodal beat notes $f_{B,0°}$ and $f_{B,90°}$ offset by 90°, producing in-phase (I) and quadrature (Q) signals. The modulation products are extracted by two additional microwave probes, recombined using a power splitter and recorded on the OSC or SA. (c) Microwave spectrum of the signal extracted from QCL_1 and acquired with the SA. The inset shows the current-voltage curve of the device and the operating point for QAM (square). (d) Demodulated microwave spectra of the I and Q channels retrieved after digital processing of the time-domain QAM waveform.

current-voltage characteristic of the QCL [inset of Fig. 2(c)]. Two additional microwave probes allow extracting the modulated beat notes from the respective positions. A 3-dB coupler is used to superimpose these two signals to produce the QAM waveform that, after an amplifier stage, is recorded with a microwave spectrum analyzer and a digital sampling oscilloscope. The microwave spectrum of the signal shows two pairs of sidebands detuned by 35 and 89 MHz from the central beat note peak [Fig. 2(c)]. We then perform software-based signal demodulation (see Section 8 in Supplement 1) that yields the original I and Q signals [Fig. 2(d)], proving that the applied I and Q tones are indeed summed in quadrature due to the phase difference of the beat note at the two positions inside the laser. This simple experiment demonstrates that a laser, a source of optical radiation, can have such unconventional functionality as to act as a microwave quadrature mixer thanks to its internal time-dependent population inversion grating. We foresee that in the future, actual digital data may be transmitted with the proposed scheme, utilizing conventional modulation schemes with complex constellations [14].

While all-electrical counterparts of the proposed device have long been commercially available and widely employed as backbones of existing communication protocols operating in the lower gigahertz range (such as Wi-Fi or 4G LTE), sources and modulators in the subterahertz and terahertz range, where future wireless communication networks are expected to operate, are an ongoing quest [15]. We emphasize that the demonstrated functionality is an inherent general feature of any QCL frequency comb and can be extended to terahertz carrier frequencies by reducing the cavity length, i.e., increasing the comb repetition rate and hence the beat note frequency. Alternatively, recent observations of self-starting harmonic frequency comb operation of QCLs where the intermodal spacing lies in the terahertz frequency band [16,17] provide a new way to generate submillimeter carriers. In the case of a harmonic frequency comb, the nature of the spatiotemporal oscillations induced by the dynamic grating of the laser remains the same as that of a fundamental frequency comb, simply corresponding to the excitation of a spatial and temporal high-order harmonic grating determined by the number of skipped modes (or free spectral ranges) in the harmonic state (Section 6F in Supplement 1). Moreover, the integration of antennas in the laser could enable wireless signal outcoupling into free space, making a QCL a unibody modulator and transmitter. The dynamic gratings of QCLs reported here thus opens up a potential route to the appearance of a new class of quadrature mixers that could be integrated into future high-speed wireless communication architectures [15].

Funding. Defense Advanced Research Projects Agency (DARPA) (W31P4Q-16-1-0002); National Science Foundation (NSF) (ECCS-1614631, DGE1144152).

Acknowledgment. We gratefully acknowledge the Lincoln Laboratory, B. Schwarz, G. Villares, D. P. Caffey, and T. Day for providing QCL devices. M. P. and D. K. wish to thank J. MacArthur and P. Horowitz for useful discussions, and T. S. Mansuripur for the initial remark on beat note extraction from a QCL that inspired this research. Any opinions, findings, conclusions, or recommendations expressed in this material are those of the authors and do not necessarily reflect the views of the Assistant Secretary of Defense for Research and Engineering or of the NSF. N. A. R. is supported by the NSF.

See the Supplement 1 for supporting content.

REFERENCES

1. A. E. Siegman, *Lasers* (University Science Books, 1986).
2. L. J. P. Ketelsen, I. Hoshino, and D. A. Ackerman, IEEE J. Quantum Electron. **27**, 957 (1991).
3. W. C. W. Fang, C. G. Bethea, Y. K. Chen, and S. L. Chuang, IEEE J. Sel. Top. Quantum Electron. **1**, 117 (1995).
4. F. Girardin and G.-H. Duan, IEEE J. Sel. Top. Quantum Electron. **3**, 461 (1997).
5. M. R. Phillips, T. E. Darcie, and E. J. Flynn, IEEE Photon. Technol. Lett. **4**, 1201 (1992).
6. A. E. Siegman, Appl. Phys. Lett. **30**, 21 (1977).
7. H. J. Eichler, P. Gunter, and D. W. Pohl, *Laser-Induced Dynamic Gratings* (Springer, 1986).
8. C. L. Tang, H. Statz, and G. Demars, J. Appl. Phys. **34**, 2289 (1963).
9. H. Choi, L. Diehl, Z.-K. Wu, M. Giovannini, J. Faist, F. Capasso, and T. B. Norris, Phys. Rev. Lett. **100**, 167401 (2008).
10. A. Hugi, G. Villares, S. Blaser, H. C. Liu, and J. Faist, Nature **492**, 229 (2012).
11. J. Faist, A. Hugi, and G. Villares, "Method and device for frequency control and stabilization of a semiconductor laser," U.S. patent WO2015059082A1 (April 30, 2015).
12. M. Rösch, G. Scalari, G. Villares, L. Bosco, M. Beck, and J. Faist, Appl. Phys. Lett. **108**, 171104 (2016).
13. Y. Wang and A. Belyanin, Opt. Express **23**, 4173 (2015).
14. A. Lapidoth, *A Foundation in Digital Communication* (Cambridge University, 2009).
15. T. Nagatsuma, G. Ducournau, and C. C. Renaud, Nat. Photonics **10**, 371 (2016).
16. T. S. Mansuripur, C. Vernet, P. Chevalier, G. Aoust, B. Schwarz, F. Xie, C. Caneau, K. Lascola, C.-E. Zah, D. P. Caffey, T. Day, L. J. Missaggia, M. K. Connors, C. A. Wang, A. Belyanin, and F. Capasso, Phys. Rev. A **94**, 063807 (2016).
17. D. Kazakov, M. Piccardo, P. Chevalier, T. S. Mansuripur, Y. Wang, F. Xie, C. En Zah, K. Lascola, A. Belyanin, and F. Capasso, Nat. Photonics **11**, 789 (2017).